PNAS
www.pnas.org

Supplementary Information for

Functional diversification of Arabidopsis SEC1-related SM proteins in cytokinetic and secretory membrane fusion

Matthias Karnahl, Misoon Park, Cornelia Krause, Ulrike Hiller, Ulrike Mayer, York-Dieter Stierhof, Gerd Jürgens

Email: gerd.juergens@zmbp.uni-tuebingen.de

This PDF file includes:

Materials and Methods
Figs. S1 to S10
Tables S1 to S6
Captions for movies S1
References for SI reference citations

Other supplementary materials for this manuscript include the following:

Movies S1

www.pnas.org/cgi/doi/10.1073/pnas.1722611115

Materials and Methods

Molecular cloning. For generating *KNOLLE::mRFP-SEC1B or KNOLLE::GFP-SEC1B, SEC1B* was amplified by PCR from the cDNA library derived from *Arabidopis thaliana* (Col) seedlings using primers sec1b-5'-SmaI and sec1b-3'-EcoRI and cloned in-frame downstream of *KNOLLE::mRFP* or *KNOLLE::GFP* cassette (*Xma*I and *EcoR*I) (1). For generating *KNOLLE::mRFP-SEC1A, SEC1A* was amplified by PCR from cDNA library using primers sec1a-5'SmaI and sec1a-3'-XbaI. The PCR product was digested with *Xma*I and *Xba*I and cloned into *Xma*I and *Avr*II-digested *KNOLLE::mRFP* cassette. For generating *KNOLLE::vYFP-KEULE*, *KEULE* from *KNOLLE::6xHA-KEULE* was PCR-amplified using primers keule 5'-XbaI and keule 3'-AvrII, digested with *Xba*I and *Avr*II and subcloned into *KNOLLE::vYFP* cassette (1, 2). For generating *pEG202::SEC1B, SEC1B* amplified from *KNOLLE::mRFP-SEC1B* with primers sec1b-*5'*-EcoRI and sec1b-3'-NotI was digested with *Eco*RI and *Not*I and cloned into the pEG202 plasmid (*Eco*RI/*Not*I). For generating *pJG4-5::SYP132, SYP132* was amplified by PCR from *KNOLLE::Myc-SYP132* (3) using primers s132-5'-EcoRI and s132-dTM-3'-SalI. The PCR product digested with *Eco*RI and *Sal*I was subcloned into the pJG4-5 plasmid (*Eco*RI/*Xho*I). For generating *pJG4-5::SYP132open,* two amino acid residues I $(Ile)_{175}$ and D $(Asp)_{176}$ within the linker domain were replaced with alanine residues by the PCR-based site-directed mutagenesis method, using primers s132-5'-SmaI and s132op-as for the N-terminal fragment and primers s132-3'-EcoRI and s132op-ss for the C-terminal fragment. Full-length *SYP132open* was generated by PCR using primers s132-5'-SmaI and s132-3'-EcoRI and the PCR product digested by *Sma*I and *Eco*RI was cloned into the *KNOLLE::Myc* cassette (*Sma*I/*Eco*RI). This engineered *SYP132open* gene was then amplified by PCR using primers s132-5'-EcoRI and s132-dTM-3'-SalI, digested with *Eco*RI and *Sal*I, and subcloned into the pJG4-5 plasmid (*Eco*RI/*Xho*I). For *pEG202::KEULE*$_{1\text{-}2a}$*SEC1B*$_{3a\text{-}2b}$ (*KS*), an N-terminal fragment was amplified from *KEULE*, using primers keu-5' and KSrev, and a complementary C-terminal fragment was amplified from *SEC1B*, using primers KSfor and sec1b-3'-NcoI. The full-length chimeric construct was generated using primers keu-5' and sec1b-3'-NcoI, digested with *Ba*mH1 and *Nco*I and subcloned into the pEG202 plasmid (*BamH*1/*Nco*I). For *pEG202::SEC1B*$_{1\text{-}2a}$*KEULE*$_{3a\text{-}2b}$ (*SK*), an N-terminal fragment was amplified from *SEC1B*, using primers sec1b-3'-EcoRI and SKrev, and a complementary C-terminal fragment was amplified from *KEULE*, using SKfor and keu-3'. The full-length chimeric construct was generated using primers sec1b-3'-EcoRI and keu-3', digested with *Eco*RI and *Nco*I and subcloned into the pEG202 plasmid (*EcoRI/*NcoI).

Genetic and transcript analysis. Identification of genetic background or transgenes was based on PCR genotyping using the following primers: for *SEC1B*, primers MK103 and MK104 (1 kb); for *sec1b*, primers MK137 and MK104 (0.5 kb); for *KNOLLE::mRFP-SEC1B*, primers RFP700-sense and MK103 (1 kb); for *KNOLLE::mRFP-SEC1A,* primers RFP700-sense and MK063 (0.9 kb); *keule*^{MM125} as reported (2, 4). Total RNA was isolated from seedlings with the RNA extraction kit (PEQlab). First strand cDNA was synthesized with RevertAid H Minus First Strand cDNA Synthesis Kit (Thermo Fisher Scientific) using an oligo (dT)18 primer. Resulting cDNA was used for PCR. See Table S6 for primer sequences.

Chemical treatment. Five-day-old seedlings were treated with 50 µM brefeldin A (BFA, 50 mM stock solution in DMSO:ethanol, Invitrogen) for 1 hr.

Pollen staining. Pollen collected from open flowers were stained with 1 µg/ml propidium iodide (PI, 1 mg/ml stock solution in H_2O, Sigma) and 2 µg/ml fluorescein diacetate (FDA, 2 mg/ml stock solution in acetone) or 1 µg/ml DAPI (1 mg/ml stock solution in H_2O) in PBS solution. After 30 min at room temperature, pollen were analyzed with a fluorescence microscope (Axiophot, Zeiss, Germany). For observation of earlier stages, anthers collected from the flower buds at various developmental stages were fixed with 4% paraformaldehyde for 1 hr and stained with DAPI for 30 min.

Co-immunoprecipitation and immunoblot analyses. The immunoprecipitation procedure was performed as reported (5). Total proteins were extracted from approximately 2 g of five-day-old seedlings in chilled buffer (50 mM Tris pH7.5, 150 mM NaCl, 1 mM EDTA, 0.5% Triton X-100) supplemented with EDTA-free protease inhibitor cocktail (Roche). 30 µl of agarose-conjugated anti-HA (mouse, Sigma-Aldrich) or anti-GFP (GFP-trap®; Chromotek) were added to cleared protein extract and incubated at 4°C for 2 hr with mild rotation. All immunoprecipitation experiments were repeated at least three times. Membranes were developed using a chemiluminescence detection system (Fusion Fx7 Imager, PEQlab, Erlangen, Germany). For immunoblot analysis of the transgenic plants, total proteins were isolated from seedlings with protein sample buffer (12 mM Tris pH6.8, 0.4% SDS, 0.01% bromophenol blue, 5% glycerol, 2.88 mM ß-mercaptoethanol) and further subjected to immunoblot analysis. For immunoblot analysis of yeast cells, total proteins were extracted from overnight-grown yeast cells by heating for 20 min at 95°C. Antibody dilutions were as follows: rabbit anti-KNOLLE serum (1:5,000) (6), rabbit anti-SYP132 serum (1:5,000) (7), rabbit anti-VAMP721/722 serum (1:5,000) (8), rabbit anti-SNAP33 serum (1:5,000) (9), rabbit anti-SYP71 serum (1:5,000) (10), rabbit anti-NPSN11 serum (1:500) (11), POD-conjugated anti-HA monoclonal antibody (1:1,000; Roche), anti-GFP monoclonal antibody (1:1,000; Roche), rat anti-RFP monoclonal antibody (1:1,000; Chromotek), rabbit anti-SEC21 serum (1:2,000; Agrisera), mouse anti-LexA (1:1,000; Santa Cruz), sheep anti-rabbit IgG-POD polyclonal antibody (1:5,000; Millipore), goat anti-mouse IgG-POD polyclonal antibody (1:5,000; Sigma).

Immunofluorescence analysis. Five-day-old seedlings were fixed with 4% paraformaldehyde solution, stored at -20°C until used and subjected to immunostaining with the following antisera: rabbit anti-KNOLLE serum (1:4,000) (6), mouse anti-HA monoclonal antibody (1:600; Roche); secondary antibodies were anti-rabbit Alexa488 (1:600, Invitrogen) and anti-mouse FITC (1:600, Dianova, Germany). For staining of nuclei, 1 µg/ml DAPI (1 mg/ml stock solution in H_2O) was used. Samples were prepared with an immunohistochemistry system (InsituPro VSi, Intavis, Cologne, Germany). For live imaging, five-day-old seedlings were used. Fluorescent images were taken using a 63x water-immersion objective in a Leica SP8 confocal laser scanning microscope. For examining SYP132::GFP-SYP132 in developing pollen, microspores were squeezed out of pollen sacs on the slide glass in MS medium and immediately observed with a Leica SP8 confocal laser scanning microscope. Line intensity profiles were measured with the Leica program.

Yeast analysis. EGY48 yeast strain was transformed with three plasmids: pSH18-34 as a LacZ reporter, pJG4-5 bearing each *Qa-SNARE* CDS indicated lacking the membrane anchor sequence and pEG202 bearing *SEC1B* or *KEULE* CDS. ß-galactosidase was quantitatively measured as previously reported with modification (2). Briefly, yeast cells were suspended in Z buffer (0.1 M Na-phosphate buffer pH 7.2, 10 mM KCl, 1 mM

MgSO4, 50 mM ß-mercaptoethanol) and followed by addition of ONPG (4 mg/ml). The formula of Miller unit was as follows: [(1000 x OD_{420})/(culture volume x time x OD_{600})] (12).

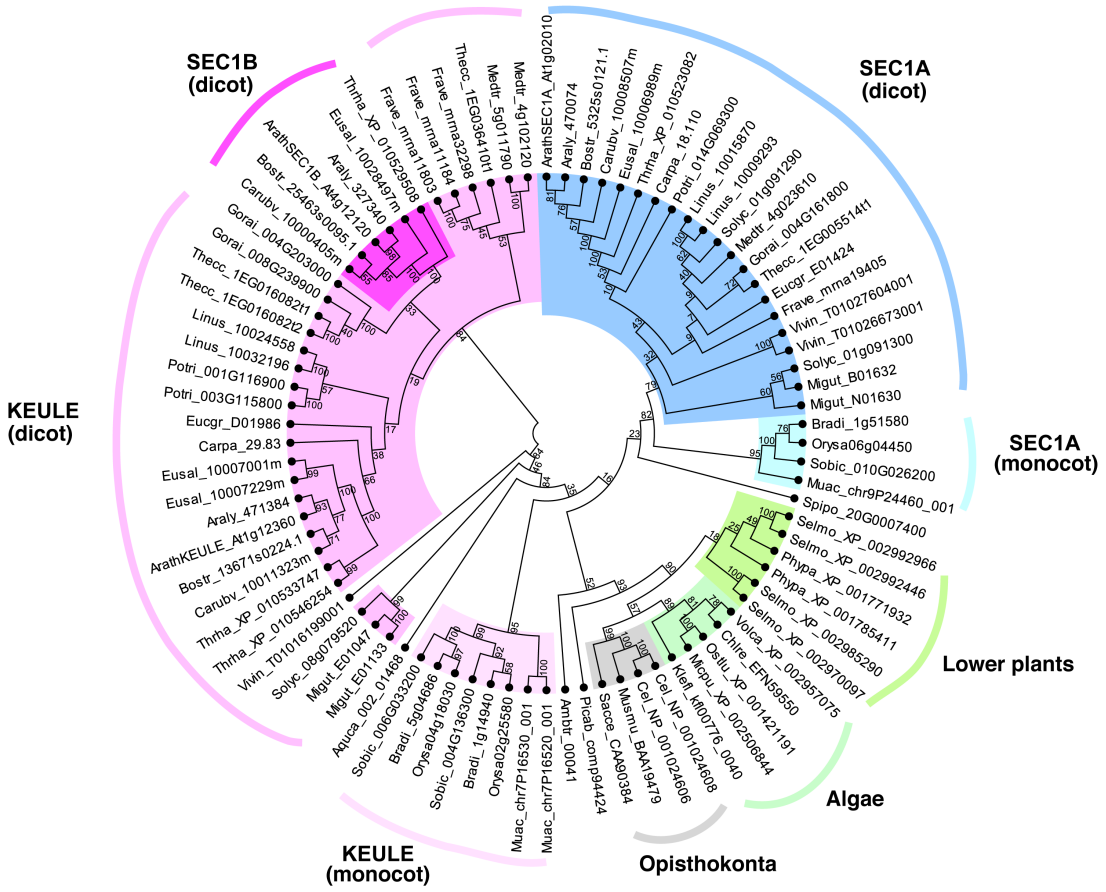

Fig. S1. Detailed unrooted phylogenetic tree of SEC1-related SM proteins and evolutionary relationship of SEC1-related paralogs in flowering plants.
The phylogenetic tree was generated using the neighbor-joining method in the CLC workbench program. The numbers at the branchpoints indicate bootstrap values for 1000 replicates. Sequences were taken from annotated plant genome resources (Phytozome 12, https://phytozome.jgi.doe.gov/pz/portal.html; https://www.ncbi.nlm.nih.gov/; http://spirodelagenome.org/jgi_csp; http://congenie.org/start; http://www.genome.jp/kegg/kegg2.html). Species analyzed: *Dicots*: Aquca, *Aquilegia caerulea*; Araly, *Arabidopsis lyrata*; Arath, *Arabidopsis thaliana*; Bostr, *Boechera stricta*; Carpa, *Carica papaya*; Carub, *Capsella rubella*; Eucgr, *Eucalyptus grandis*; Eusal, *Eutrema salsugineum* (= *Thellungiella halophila*); Frave, *Fragaria vesca*; Gorai, *Gossypium raimondii*; Linus, *Linum usitatissimum*; Medtr, *Medicago trunculata*; Migut, *Mimulus guttatus*; Potri, *Populus trichocarpa*; Solyc, *Solanum lycopersicum*; Tarha, *Tarenaya* (= Cleome) *hassleriana*; Thecc, *Theobroma cacao*; Vivin, *Vitis vinifera*. *Monocots*: Bradi, *Brachipodium distachyon*; Muac, *Musa acuminata*; Orysa, *Oryza sativa*; Sobic, *Sorghum bicolor*; Spipo, *Spirodela polyrhiza*. *Basal angiosperm*: Ambtr, *Amborella trichpoda*. *Gymnosperm*: Picab, *Picea abies*. *Lower plants*: Phypa, *Physcomitrella patens* (bryophyte); Selmo, *Selaginella moellendorffii* (lycopod). *Algae*: Chlre, *Chlamydomonas reinhardtii*; Klefl, *Klebsormidium flaccidum*; Micpu, *Micromonas pusilla*; Ostlu, *Ostreococcus lucimarinus*; Volca, *Volvox carteri*. *Opisthokonts*: Cel, *Caenorhabditis elegans*; Musmu, *Mus musculus*; Sacce, *Saccharomyces cerevisiae*.

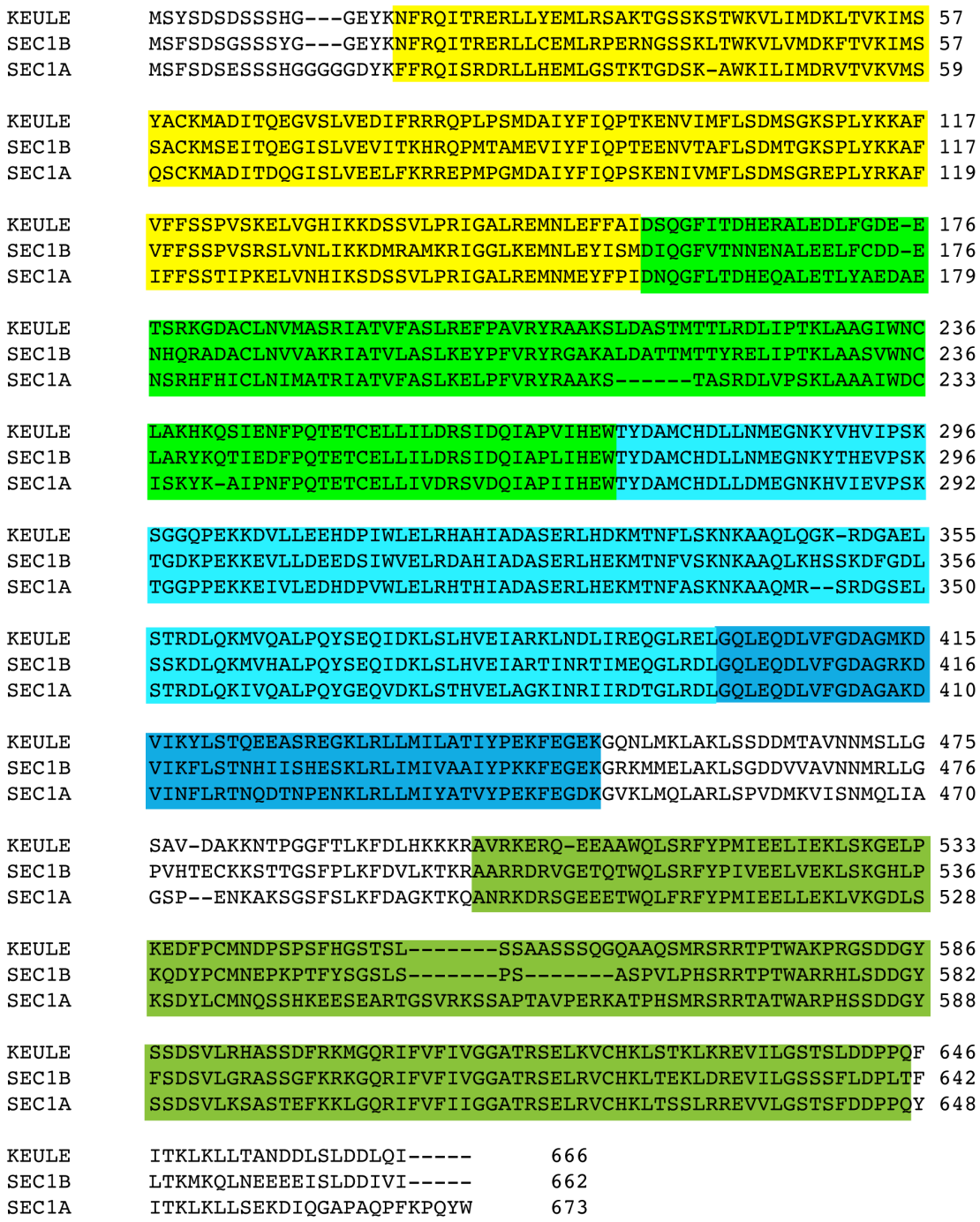

Fig. S2. Sequence alignment of *Arabidopsis thaliana* SM proteins. Peptide sequences of KEULE (At1g12360), SEC1A (At1g02010) and SEC1B (At4g12120) were aligned in Clustal Omega (1.2.4). Domains were determined from the sequence comparison with mammalian SEC1, Munc18-1 and Munc18c (13): yellow, domain 1; bright green, domain 2a; bright blue, domain 3a; dark blue, domain 3b; dark green, domain 2b. Numbers indicate amino acid residues.

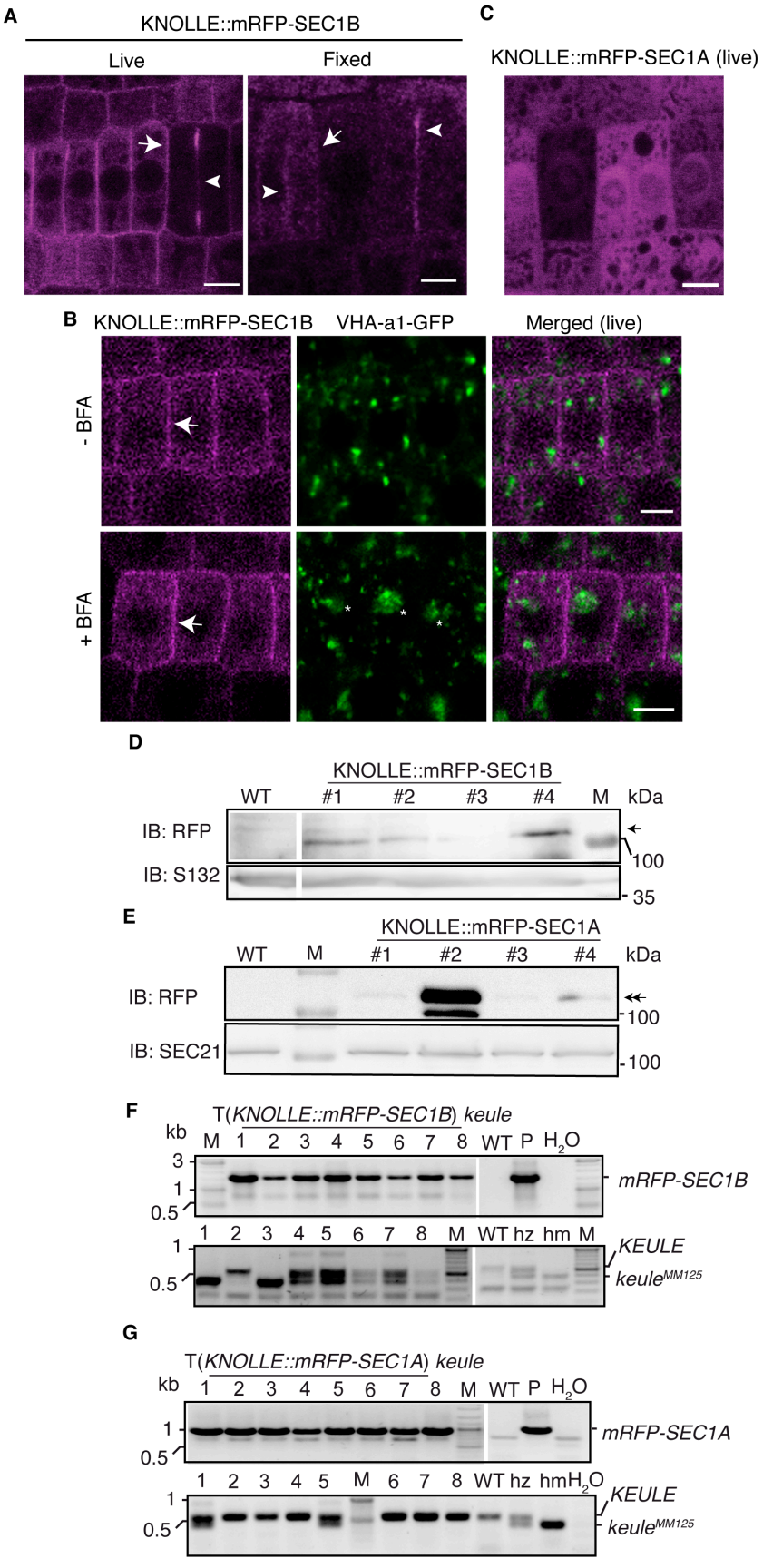
A
KNOLLE::mRFP-SEC1B
Live
Fixed
C
KNOLLE::mRFP-SEC1A (live)
B
KNOLLE::mRFP-SEC1B
VHA-a1-GFP
Merged (live)
- BFA
+ BFA
D
KNOLLE::mRFP-SEC1B
WT
#1
#2
#3
#4
M
kDa
IB: RFP
IB: S132
100
35
E
KNOLLE::mRFP-SEC1A
WT
M
#1
#2
#3
#4
kDa
IB: RFP
IB: SEC21
100
100
F
T(KNOLLE::mRFP-SEC1B) keule
kb
M 1 2 3 4 5 6 7 8 WT P H2O
3
1
0.5
mRFP-SEC1B
1 2 3 4 5 6 7 8 M WT hz hm M
1
0.5
KEULE
keuleMM125
G
T(KNOLLE::mRFP-SEC1A) keule
kb
1 2 3 4 5 6 7 8 M WT P H2O
1
0.5
mRFP-SEC1A
1 2 3 4 5 M 6 7 8 WT hz hmH2O
1
0.5
KEULE
keuleMM125

Fig. S3. Subcellular localization of SEC1B and SEC1A and analysis of transgenic *SEC1B* and *SEC1A* lines tested for rescue of *keule* mutant. (**A**) Confocal images of single channel of KNOLLE::mRFP-SEC1B in live (*left*) or fixed (*right*) seedling roots. (**B**) Confocal images KNOLLE::mRFP-SEC1B after BFA treatment. Note that mRFP-SEC1B is insensitive to BFA whereas VHA-a1-GFP, a TGN-resident protein, accumulates in the BFA bodies (asterisks) upon BFA treatment. (**C**) Confocal image of single channel of KNOLLE::mRFP-SEC1A in live seedling root. Note that mRFP-SEC1A is mainly dispersed in the cytosol unlike mRFP-SEC1B and HA-KEULE (see Fig. 2A). Arrows and arrowheads indicate plasma membrane and cell plate, respectively (**A**, **B**). Scale bars, 10 μm (**A**-**C**). (**D**, **E**) Immunoblot analyses of KNOLLE::mRFP-SEC1B (**D**) and KNOLLE:mRFP-SEC1A (**E**) expression. Protein extracts from wild type (WT) and T2 seedlings from four independent transgenic lines were subjected to immunoblot analysis with indicated antisera. SYP132 (S132; **D**) and SEC21 (aka γCOP, **E**) were used as loading controls. RFP, anti-RFP; S132, anti-SYP132; SEC21, anti-SEC21 antisera. M, molecular weight markers; molecular weight (kDa, kilodaltons) indicated on the right. Arrow, mRFP-SEC1B (**D**); double-headed arrow, mRFP-SEC1A (**E**). (**F**, **G**) Complementation tests of *KNOLLE::mRFP-SEC1B* (**F**) and *KNOLLE::mRFP-SEC1A* (**G**) transgenes in *keule* mutant. Genomic DNA was isolated from individual wild type-looking seedlings in T2 progenies and subjected to PCR for the transgenes (upper panel in ***F***, *mRFP-SEC1B*; upper panel in ***G***, *mRFP-SEC1A*) and for the endogenous *KEULE* genotypes (lower panels, 0.5 kb and 0.4 kb bands represent *KEULE* and $keule^{MM125}$ alleles, respectively). Note that seedlings *1* and *3* are fully rescued (**F**) but none in (**G**). T, transgene; P, positive control; hz, *keule* heterozygote; hm, *keule* homozygote; H_2O, control without template; M, molecular marker (kb, kilobases); WT, wild-type. See Table S1 for quantitative analysis of complementation tests.

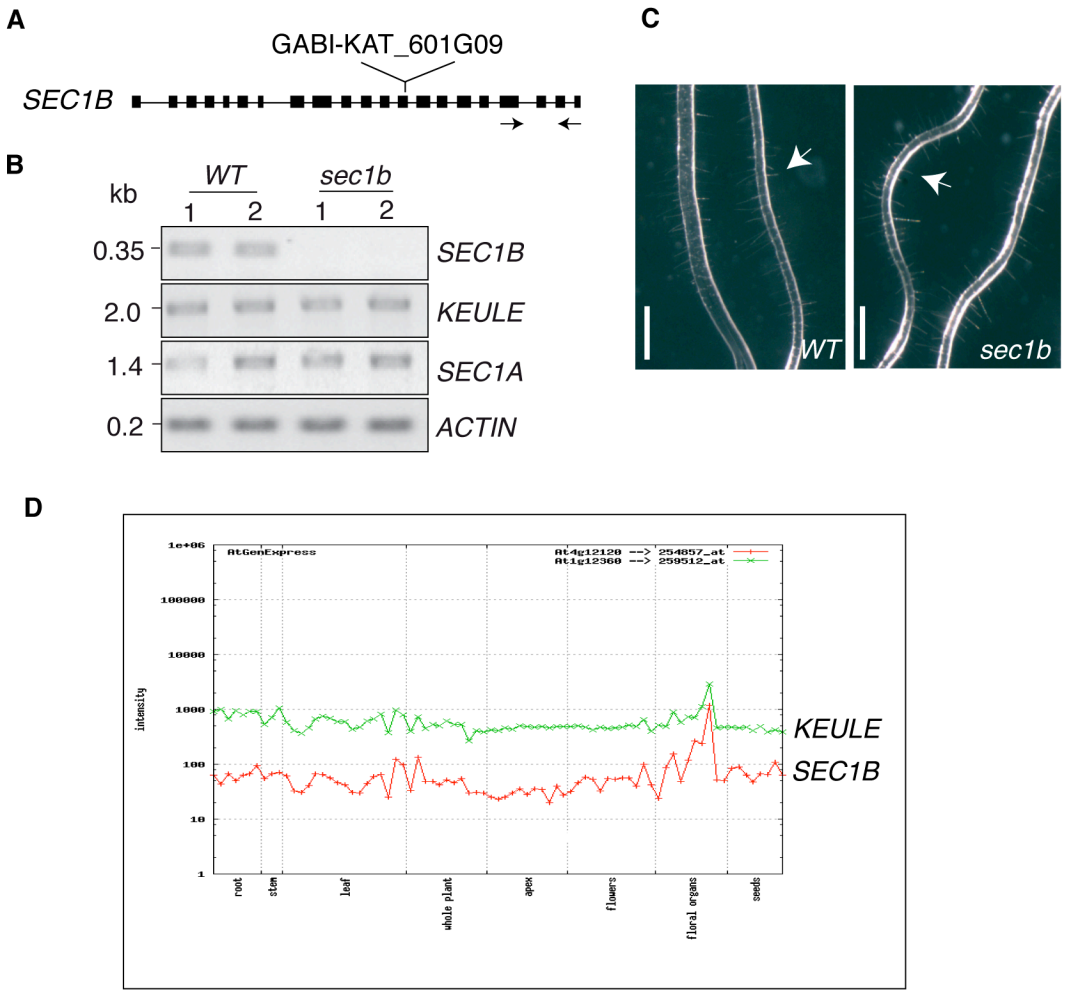

Fig. S4. Analysis of *sec1b* T-DNA insertion line, mutant phenotype and expression profile. (**A**) Diagram of the single T-DNA insertion (GABI-KAT_601G09) in the 13th exon of the *SEC1B* gene. Arrows indicate the position of the primers used for RT-PCR analysis. (**B**) RT-PCR analysis of *sec1b*. cDNAs were synthesized from total transcripts of wild-type (*WT*) and *sec1b* mutant seedlings. *ACTIN* was used as control. Numbers (*left*), molecular weight (kb, kilobases). Note that there is no compensatory up-regulation of *KEULE* or *SEC1A* expression in the *sec1b* mutant. (**C**) Roots of 6-day-old *sec1b* mutant seedling and wild-type (WT). Note that root hairs (arrows) in *sec1b* appear indistinguishable from wild type. Scale bars, 0.5 mm (**C**). (**D**) Expression profiles of Arabidopsis *KEULE* (At1g12360, green) and *SEC1B* (At4g12120, red) in AtGenExpress visualization tool (14; http://jsp.weigelworld.org/expviz/expviz.jsp). Note that expression profile of *SEC1A* (At1g02010) is not available.

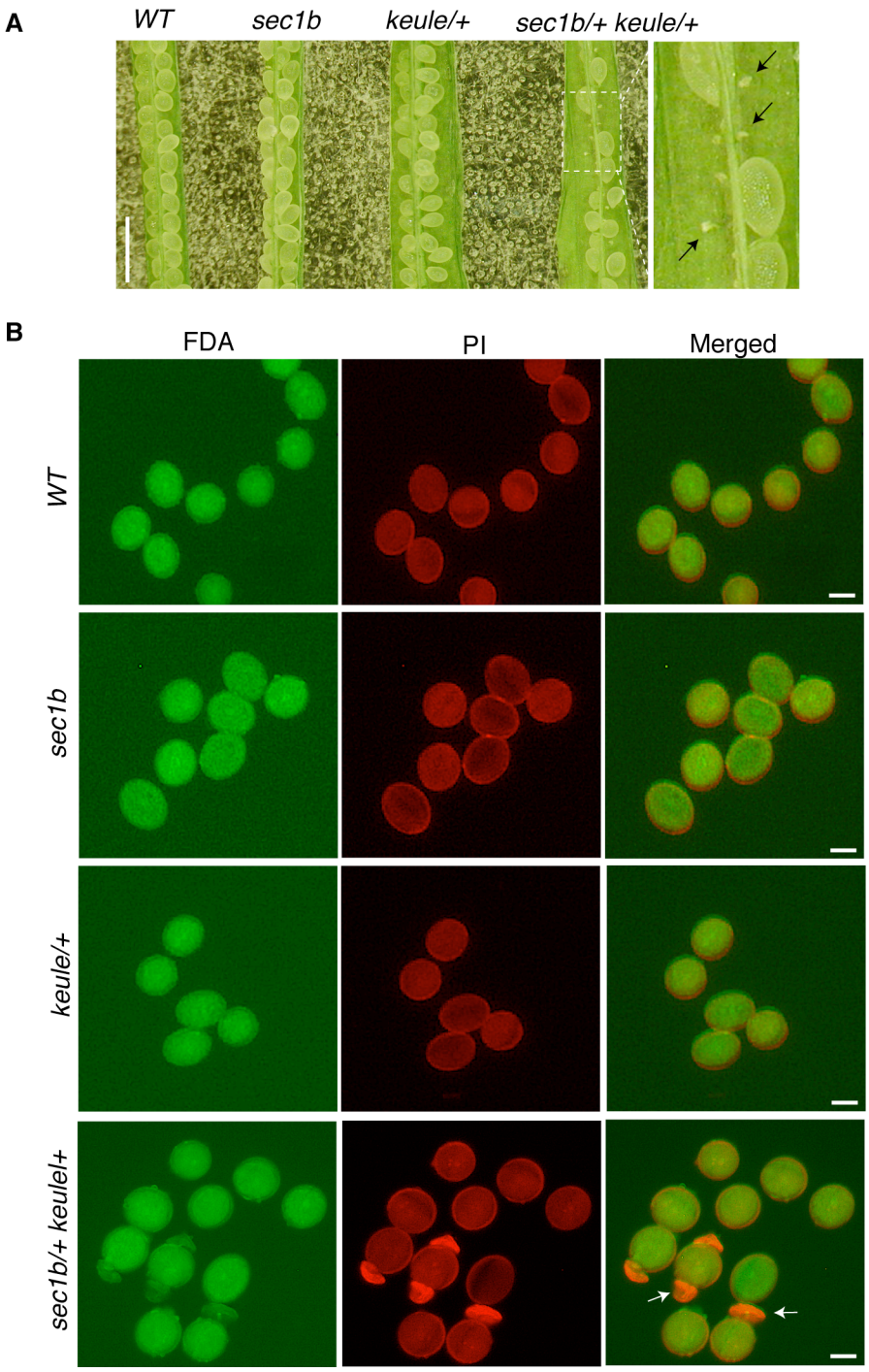

Fig. S5. **Reproductive phenotypes of *sec1b/+ keule/+* doubly heterozygous plants.** (**A**) Ovules in open siliques from selfed wild-type (*WT*), *sec1b* mutant, *keule/+* heterozygous and *sec1b/+ keule/+* doubly heterozygous plants. Note many unfertilized ovules (arrows) in silique from *sec1b/+ keule/+* doubly heterozygous plant. See Table S2A for quantitative analysis. (**B**) Pollen viability analysis. Mature pollen were stained with fluorescein diacetate (FDA, green) and propidium iodide (PI, red). Note that *sec1b/+ keule/+* doubly heterozygous plants produce inviable pollen, which are collapsed and strongly stained with PI. See Table S2C for quantitative analysis. Scale bars, 1 mm (**A**), 10 μm (**B**).

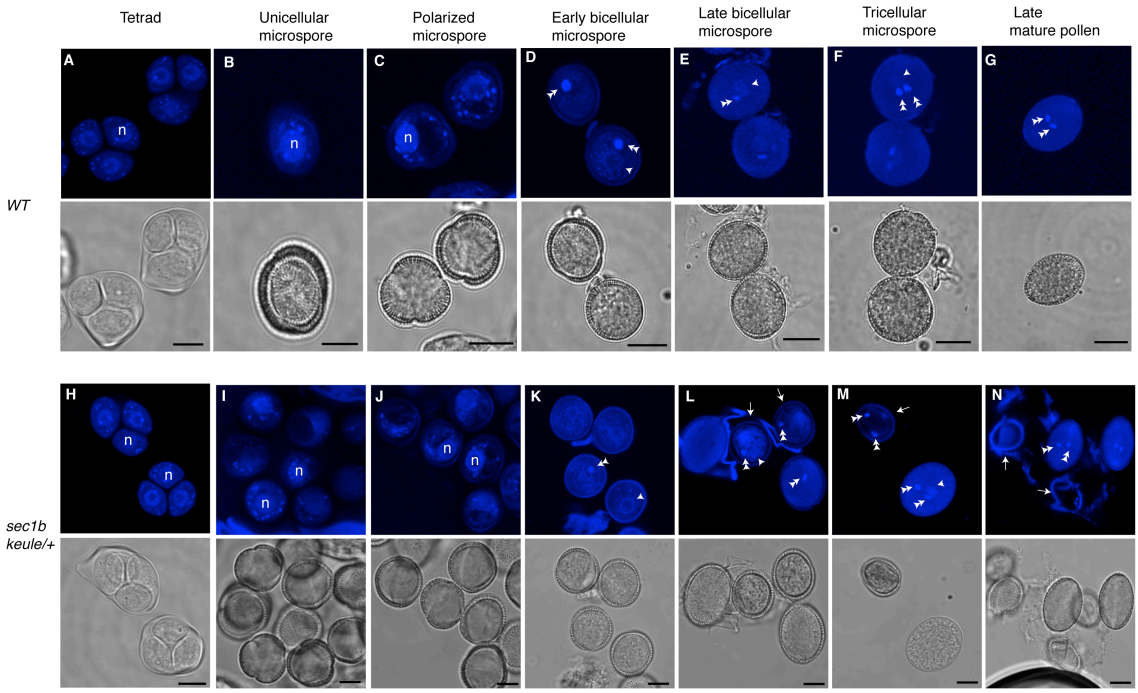

Fig. S6. **DAPI-stained developing pollen of *sec1b keule/+* double mutant**. Anthers of wild-type *(WT)* or *sec1b keule/+* plants were harvested at the indicated stages and after fixation stained with DAPI (blue) for visualization of nuclei. Note that *sec1b keule* double mutant pollen are indistinguishable from *WT* until the bicellular stage and that *sec1b keule* double mutant pollen comprise two sperm cells and one vegetative cell like wild-type at the tricellular stage, although double-mutant pollen collapsed at the late stages (arrows in **L**-**N**). Double-headed arrowheads, generative cells; arrowheads; vegetative cells; n, haploid nucleus. Scale bars, 10 μm.

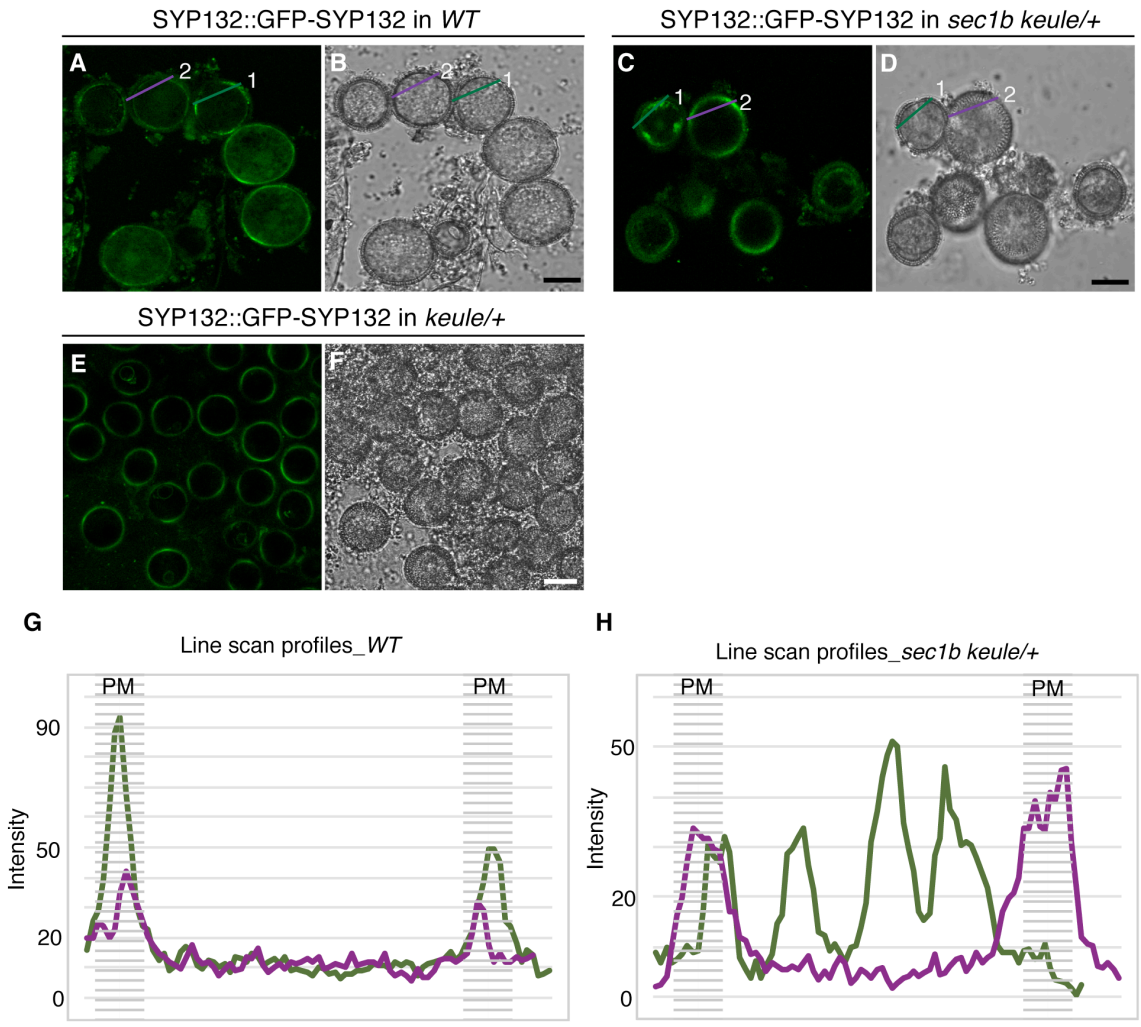

Fig. S7. Localization of SYP132 in developing *sec1b keule* double mutant pollen. (**A**-**F**) Localization of SYP132::GFP-SYP132 in wild-type (*WT*, **A**, **B**), *sec1b keule/+* (**C, D**) or *keule/+* (**E**, **F**) microspores at unicellular or bicellular stage. (**A, C, E**) GFP-fluorescence images. (**B**, **D, F**) Bright-field images to indicate pollen morphology. Note that GFP-SYP132 in *sec1b keule* mutant was present in larger aggregates in the cytosol while GFP-SYP132 in WT mainly located at the plasma membrane (PM). (**G**, **H**) Line scan profiles. Signal intensity of GFP-SYP132 was measured along lines indicated in (**A**-**D**): line 1, green color; line 2, purple color. Line profile of line 2 in (**C**, **D**) representing the GFP signal in the *sec1b* single mutant was shown for comparison (**H**). Note that the GFP signal in *sec1b keule* double mutant is largely intracellular (green, **H**) whereas the signal in *WT* or *sec1b* single mutant is highest at the plasma membrane (PM; dashed lines in **G**, **H**). See Table S3 for quantitative measurement. Scale bars, 10 μm (**B**, **D, F**).

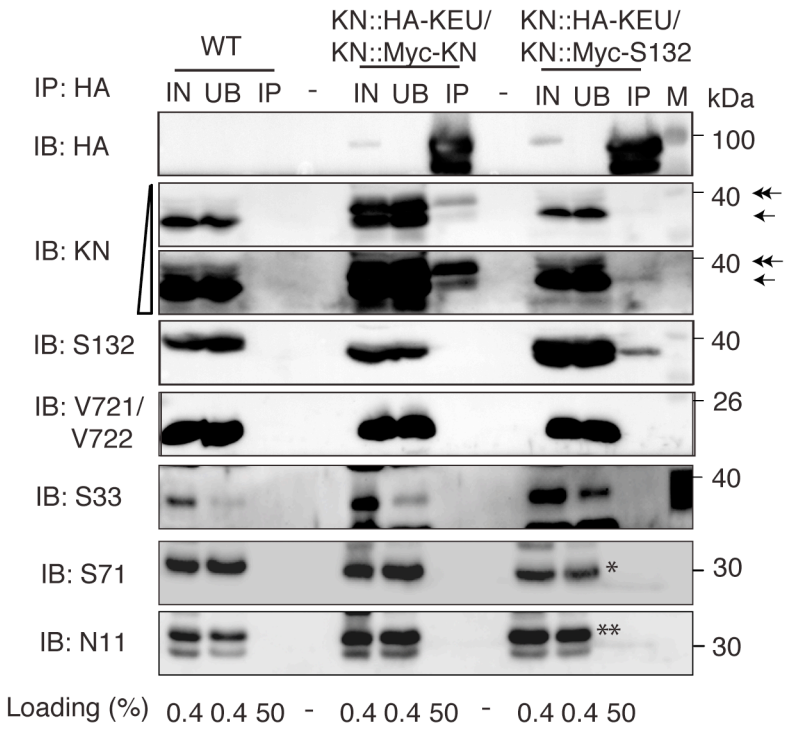

Fig. S8. **Co-immunoprecipitation analysis of SEC1-like SM proteins and SYP1 Qa-SNAREs.** Protein extracts from *KNOLLE::6xHA-KEULE* (KN::HA-KEU) seedlings expressing *KNOLLE::Myc-KNOLLE* (KN::Myc-KN) or *KNOLLE::Myc-SYP132* (KN::Myc-S132) were subjected to immunoprecipitation with anti-HA beads. Wild type (WT, Col) seedlings were used as control. Immunoprecipitates (IP) were immunoblotted (IB) with the antisera indicated: HA, anti-HA; KN, anti-KNOLLE; S132, anti-SYP132; V721/V722, anti-VAMP721/V722; S33, anti-SNAP33; S71, anti-SYP71; N11, anti-NPSN11. Arrows, endogenous KNOLLE; double-headed arrows, Myc-KNOLLE; asterisk, SYP71; double asterisks, NPSN11. IN, input; UB, unbound; M, molecular markers (size in kDa). Loading (%), relative loading volume to total volume.

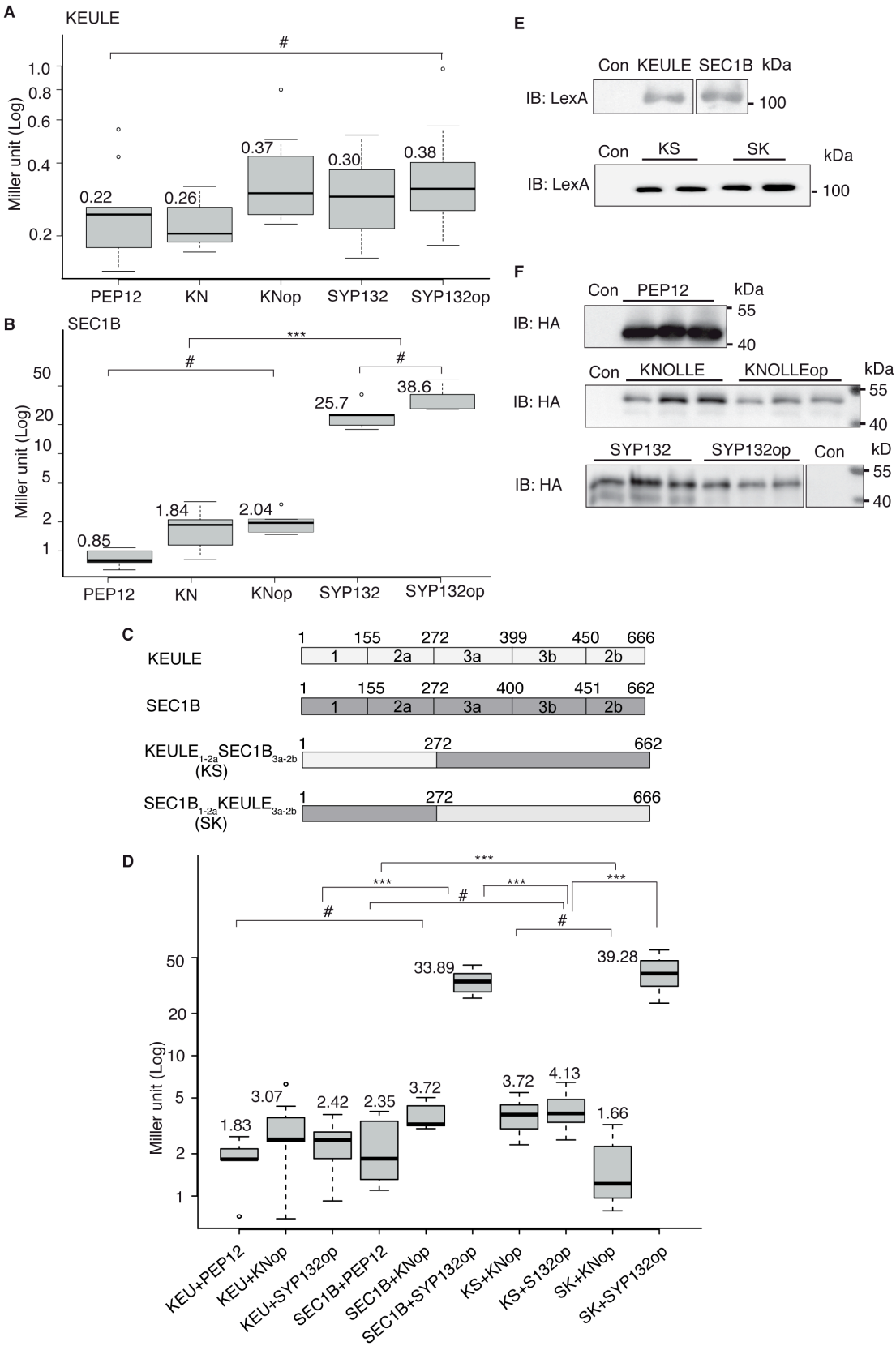
A
KEULE
Miller unit (Log)
PEP12
KN
KNop
SYP132
SYP132op
B
SEC1B
C
KEULE
SEC1B
KEULE1-2aSEC1B3a-2b (KS)
SEC1B1-2aKEULE3a-2b (SK)
D
KEU+PEP12
KEU+KNop
KEU+SYP132op
SEC1B+PEP12
SEC1B+KNop
SEC1B+SYP132op
KS+KNop
KS+S132op
SK+KNop
SK+SYP132op
E
Con KEULE SEC1B kDa
IB: LexA
Con KS SK kDa
F
Con PEP12 kDa
IB: HA
Con KNOLLE KNOLLEop kDa
SYP132 SYP132op Con

Fig. S9. **Semi-quantitative β-galactosidase assay in yeast**. (**A**, **B**) Boxplots of ß-galactosidase activity. Yeast cells expressing BD-KEULE (**A**) or BD-SEC1B (**B**) were transformed with AD plasmids coding for the indicated Qa-SNAREs. KNOLLEop, open form of KNOLLE ($IE_{182,183}AA$); SYP132op, open form of SYP132 ($ID_{175, 176}AA$). Note that mutations in the linker region adjacent to the SNARE domain prevent backfolding of N-terminal helices onto SNARE domain, rendering the SNARE constitutively open (2). PEP12 was used as control. Note that the C-terminal membrane anchor was deleted to render the Qa-SNAREs soluble. Y axis, Miller units (Log). Experiments were repeated at least three times. Box-associated numbers, sample means. Statistical analysis with single-factor ANOVA ((**A**) $F_{42,4} = 1.766$, $p = 0.154$; (**B**) $F_{4,20} = 32.31$, $p < 0.0001$) and posteriori Tukey test (#, p>0.1; ***, p< 0.0001 in **A** and **B)** (**C**, **D**) Analysis of swap mutants of KEULE and SEC1B. (**C**) Diagram of swap mutants of KEULE and SEC1B (see Fig. S2 for the sequences). (**D**) Boxplot of ß-galactosidase assay. Y axis, Miller units. Experiments were repeated at least two times. Box-associated numbers, sample means. Statistical analysis with two-way ANOVA ($F_{89,4} = 93.79$; p <2e-16) and posteriori Tukey test (#, p>0.1; ***p< 0.0001). (**E, F**) Expression analyses of fusion proteins tested for interaction (BD fusions, **E**; HA-tagged AD fusions, **F**). Protein lysates of yeast cells expressing the indicated proteins were subjected to immunoblot (IB) analysis with antisera. LexA, anti-lexA; HA, anti-HA. Con, yeast cells bearing empty vectors. Numbers (right), molecular weight (kDa, kilodaltons).

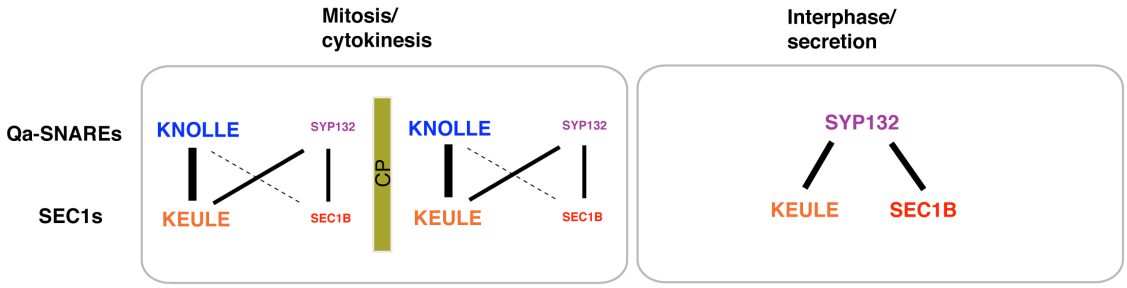

Fig. S10. Scheme depicting the interactions of SEC1-related SM proteins SEC1B and KEULE with SYP1 Qa-SNAREs KNOLLE and SYP132 in cytokinesis and in secretory traffic during interphase. In mitotic cells (*left*), KEULE predominantly interacts with KNOLLE and less with SYP132 whereas SEC1B mainly interacts with SYP132 and hardly with KNOLLE in cell-plate (CP) formation during cytokinesis (dashed line). In interphase cells (*right*), both KEULE and SEC1B contribute equally to membrane fusion in secretion by interacting with SYP132 at the plasma membrane.

Table S1. Complementation tests for *keule* rescue by *SEC1* transgenes

T1 plants		T2 seedlings				
Transgenes	alleles	PPTres	PPTsens	WT	[*]*keule*	N
-	*keule*/+	-	-	82% (339)	[#]18% (72)	411
KN::mRFP-SEC1B #1	*keule*/+	73% (153)	25% (52)	98% (205)	2% (5)	210
KN::mRFP-SEC1B #2	*keule*/+	74% (276)	19% (71)	93% (347)	7% (24)	371
KN::mRFP-SEC1B #3	*keule*/+	76% (376)	20% (100)	96% (476)	4% (20)	496
KN::mRFP-SEC1A #1	*keule*/+	62% (216)	23% (79)	85% (295)	15% (54)	349
KN::mRFP-SEC1A #2	*keule*/+	58% (629)	23% (253)	81% (882)	19% (206)	1088
KN::mRFP-SEC1A #3	*keule*/+	67% (228)	15% (50)	82% (278)	18% (62)	340

PPTres, phosphinotricin-resistant (marker for the transgene); PPTsens, PPT-sensitive.
[*]In theory, if a single-copy transgene rescues the *keule* mutant the percentage of *keule* homozygotes will be 6.25% rather than 25%.
[#]Note that the *keule*/+ parental line segregates less than the theoretically expected 25% *keule* homozygous offspring.

Table S2. Genetic analysis of *sec1b keule* double mutant

A. Quantitative analysis of unfertilized ovules in *sec1b/+ keule/+* doubly heterozygous plants

	Ovule phenotype		
Plant genotype	Normal	Unfertilized	N
WT (Col)	96% (148)	4% (6)	154
sec1b/+	95% (161)	5% (8)	169
keule/+	95% (113)	5% (6)	119
sec1b/+ keule/+ #1	41% (100)	59% (143)	243
sec1b/+ keule/+ #2	42% (237)	58% (325)	562
**sec1b/+ keule/+* x *WT*	30% (261)	70% (607)	868

* The doubly heterozygous plants were pollinated by wild-type plants.

B. Transmission of *sec1b keule* double mutant

	F1 genotypes				
Parental cross (female x male)	*SEC1B/+ KEULE/+*	*sec1b/+ KEULE/+*	*SEC1B/+ keule/+*	*sec1b/+ keule/+*	N
sec1b/+ keule/+ x *WT*	25% (30)	27% (31)	41% (48)	7% (8)	117
WT x *sec1b/+ keule/+*	33% (36)	32% (34)	33% (35)	2% (2)	107

Doubly heterozygous plants were crossed with wild-type plants reciprocally. Resultant F1 seedlings were genotyped. In theory, each F1 genotype amounts to 25%.

C. Pollen viability of *sec1b+ keule/+* doubly heterozygous plants

	Pollen phenotype		
Plant genotype	Live pollen	Dead pollen	N
WT (Col)	100% (145)	0% (0)	145
sec1b	100% (271)	0% (0)	271
keule/+	100% (60)	0% (0)	60
sec1b/+ keule/+	75% (295)	25% (99)	394

Table S3. Localization of SYP132::GFP-SYP132 in developing *sec1b keule* double mutant pollen

	Localization of GFP signal		
Genotype of plant	Plasma membrane	Aggregates in the cytoplasm	N
WT	95% (93)	5% (5)	98
**sec1b keule/+*	53% (81)	47% (71)	152

This was counted from the snapshot images randomly taken.
*In theory, 50% of developing pollen are *sec1b keule* double mutant and 50% are *sec1b* single mutant.
See also Figure 3D and Figure S7 for images and line intensity profiles.

Table S4. Genetic analysis of SEC1-Qa SNARE double mutants

A. Phenotypic segregation ratio of *syp132^{tam} keule* double mutant

	F1 embryo phenotypes			
Parental cross (female x male)	#WT	#*keule*	**syp132^{tam} keule*	N
(*syp132$^{T\text{-}DNA}$/SYP132 syp132^{amiR}/- keule/+*) x (*syp132$^{T\text{-}DNA}$/SYP132 RPS5A::GAL4/- keule/+*)	83% (724)	12% (107)	5% (44)	875

*Note that *syp132^{tam}* mutant is a combination of *syp132$^{T\text{-}DNA}$* allele and artificial microRNA against *SYP132* (*syp132^{amiR}*) expressed with the *GAL4>>UAS* expression system, using the strong *RPS5A* promoter (7). See Figure 5H for embryo image.
#Note that the embryo phenotype of *syp132$^{T\text{-}DNA}$* or *syp132^{amiR}* is indistinguishable from wild type. In addition, *syp132^{tam}* resembles the *keule* single mutant phenotypically (7).

B. Segregation ratio of *knolle sec1b* double mutant

	F1 embryo phenotypes			
Parental genotype	WT	*knolle*	#*knolle sec1b*	N
knolle/+	78% (213)	22% (60)	none	273
sec1b/+ knolle/+ #1	80% (265)	14% (45)	6% (21)	331
sec1b/+ knolle/+ #2	76% (253)	18% (60)	6% (22)	335

See Figure 5F for embryo image.

C. Phenotypic segregation ratio of *syp132^{tam} sec1b* double mutant

	F1 seedling phenotypes				
Parental cross (female x male)	WT	*syp132$^{T\text{-}DNA}$*	*syp132^{amiR}*	#*syp132^{tam} sec1b*	N
(*syp132$^{T\text{-}DNA}$/SYP132 syp132^{ami}/- sec1b/+*) x (*syp132$^{T\text{-}DNA}$/SYP132 sec1b/+ RPS5A::GAL4/-*)	50% (44)	20% (18)	24% (21)	6% (5)	88
(*syp132$^{T\text{-}DNA}$/SYP132 syp132^{ami}/- sec1b/+*) x (*syp132$^{T\text{-}DNA}$/SYP132 sec1b/+ RPS5A::GAL4/-*)	61% (57)	13% (12)	19% (18)	7% (7)	94

See Figure 5J and K for images. The double mutant cannot be phenotypically distinguished from the *syp132^{tam}* mutant.

Table S5. Transmission analysis of SEC1-Qa SNARE double mutants

A. Transmission analysis of *knolle sec1b* double mutant

	F1 genotypes				
Parental cross (female x male)	*KNOLLE/+ SEC1B/+*	*knolle/+ SEC1B/+*	*KNOLLE/+ sec1b/+*	*knolle/+ sec1b/+*	N
knolle/+ sec1b/+ x *WT*	21% (41)	16% (32)	34% (68)	29% (59)	200
WT x *knolle/+ sec1b/+*	28% (57)	25% (51)	27% (55)	19% (38)	201

Doubly heterozygous plants were crossed with wild-type plants reciprocally. Resultant F1 seedlings were genotyped. In theory, each genotype would amount to 25% if there is no defect in transmission.

B. Transmission analysis of *syp132$^{T\text{-}DNA}$ sec1b* double mutant

	F1 seedling phenotypes		
Parental cross (female x male)	PPTres	PPTsen	N
syp132$^{T\text{-}DNA}$/SYP132 sec1b/+ x *WT*	*51% (165)	49% (167)	332
WT x *syp132$^{T\text{-}DNA}$/SYP132 sec1b/+*	**39% (184)	61% (287)	471

Doubly heterozygous plants were crossed with wild-type plants reciprocally. Resultant F1 were germinated on the PPT-containing media. In theory, 50% are PPT-resistant (bearing a *syp132* T-DNA insertion either in wild-type or *sec1b/+* background) if there is no defect in transmission. Randomly selected approximately 50 PPT-resistant seedlings were individually genotyped for verification:
*29% were *syp132$^{T\text{-}DNA}$/SYP132 SEC1B/+* and 22% were *syp132$^{T\text{-}DNA}$/SYP132 sec1b/+*;
**30% were *syp132$^{T\text{-}DNA}$/SYP132 SEC1B/+* and 9% were *syp132$^{T\text{-}DNA}$/SYP132 sec1b/+*.

C. Transmission analysis of *syp132$^{T\text{-}DNA}$ keule* double mutant

	F1 seedling phenotypes		
Parental cross (female x male)	PPTres	PPTsen	N
syp132$^{T\text{-}DNA}$/SYP132 keule/+ x *WT*	*50% (503)	50% (498)	1001
WT x *syp132$^{T\text{-}DNA}$/SYP132 keule/+*	**55% (1000)	45% (802)	1802

Doubly heterozygous plants were crossed with wild-type plants reciprocally. Resultant F1 were germinated on the PPT-containing media. In theory, 50% are PPT-resistant (bearing a *syp132* T-DNA insertion either in wild-type or *keule/+* background) if there is no defect in transmission. Randomly selected 50 PPT-resistant seedlings were individually genotyped for verification:
*21% in *syp132$^{T\text{-}DNA}$/SYP132 KEULE/+* and 28% in *syp132$^{T\text{-}DNA}$/SYP132 keule/+*;
**24% in *syp132$^{T\text{-}DNA}$/SYP132 KEULE/+* and 31% in *syp132$^{T\text{-}DNA}$/SYP132 keule/+*.

Table S6. Sequences of primers used

primers	sequence 5' – 3'	remark
GABI-LBs	ATATTGACCATCATACTCATTGC	genotyping (*sec1b*)
MK103	GTTGTGCTCTTTTTGCACTCC	genotyping (*SEC1B*)
MK104	CACACACGAGGTGACATTTTG	genotyping (*SEC1B*)
MK063	CGTGTATGATAGGAGCGATC	genotyping (*SEC1A*)
RFP700-sense	CAAGACCGACATCAAGCTGGA	genotyping (*RFP)*
s1b-RT-ss	GCCAACCTTTTATTCTGGCTC	RT-PCR (*SEC1B*)
s1b-RT-as	GATTCTCAAATGACAATATCATCAAGTGAGATCTCCT	RT-PCR (*SEC1B*)
keu-ss	AAAAAAGGATCCAAATGTCGTACTCTGACTCC	RT-PCR (*KEULE*)
keu-as	TTTTTTGTCGACTCATATTTGGAGATCGTCTAA	RT-PCR (*KEULE*)
s1a-RT-ss	AGAAAGCTGGGTCGAATTCCGTGAAAGGCGATCTAT	RT-PCR (*SEC1A*)
s1a-RT-as	AACTCGAGTCACCAGTATTGTGGTTTGAAGGG	RT-PCR (*SEC1A*)
act-ss	ATTCAGATGCCCAGAAGTCTT	RT-PCR (*ACTIN*)
act-as	GCAAGTGCTGTGATTTCTTTG	RT-PCR (*ACTIN*)
sec1b-5'-AvrII	AAACCTAGGATGTCCTTCTCCGATTCTGG	cloning (*RFP-SEC1B*)
sec1b-3'-NotI	AAGCGGCCGCTCAAATGACAATATCATCAAGTGAG	cloning (*RFP-SEC1B*)
sec1b-5'-SmaI	AACCCGGGATGTCCTTCTCCGATTCTGG	cloning (*RFP-SEC1B*)
sec1b-3'-EcorI	AAGAATTCTCAAATGACAATATCATCAAGTGAGATCT	cloning (*RFP-SEC1B*)
sec1b-5'-EcoRI	AAGAATTCATGTCCTTCTCCGATTCTGGATC	cloning (*SEC1B*)
GFP-AttB1-5	AAAAAGCAGGCTATATGGTGAGCAAGGGCG	cloning (*GFP-SEC1B*)
pSK-3'-AttBI	AGAAAGCTGGGTCTCCACCGCGGTGGC	cloning (*GFP-SEC1B*)
sec1a-5'-AvrII	AAACCTAGGATGTCGTTCTCCGATTCAGAGTC	cloning (*RFP-SEC1A*)
sec1a-3'-NotI	AAGCGGCCGCTCACCAGTATTGTGGTTTGAAGGG	cloning (*RFP-SEC1A*)
sec1a-5'-SmaI	AACCCGGGATGTCCTTCTCCGATTCTGG	cloning (*RFP-SEC1A*)
sec1a-3'-XbaI	AATCTAGATCACCAGTATTGTGGTTTGAAGG	cloning (*RFP-SEC1A*)
keule 5'-XbaI	AAAATCTAGAATGTCGTACTCTGACTCC	cloning (*vYFP-KEULE*)
keule 3'-AvrII	TTTTCCTAGGTCATATTTGGAGATCGTCTAA	cloning (*vYFP-KEULE*)
s132-5'-EcoRI	AAAAAAGAATTCATGAACGATCTTCTGAAGGGT	cloning (*SYP132*)
s132-dTM-3'-SalI	AAGTCGACCTACATCCATTTTCTTGAGTTCTTCTGC	cloning (*SYP132*)
s132-5'-SmaI	AAACCCGGGATGAACGATCTTCTGAAGGGTTC	cloning (*SYP132*open)

s132op-as	CAATTCAGCAGCAGTATCTTCATCCGCCC	cloning (*SYP132*open)
s132op-ss	GAAGATACTGCTGCTGAATTGATTGAAACTGGAAAC	cloning (*SYP132*open)
s132-3'-EcoRI	AAAGAATTCTCAAGCACTCTTGTTTTTCCAA	cloning (*SYP132*open)
keu-5'	AAAAAAGGATCCAAATGTCGTACTCTGACTCC	cloning (*KS*)
keu-3'	TTTTTCCATGGTCATATTTGGAGATCGTCTAA	cloning (*SK*)
sec1b-3'-NcoI	TTTTTCCATGGTCAAATGACAATATCATCAAG	cloning (*KS*)
KSfor	CCTGTTATACATGAGTGGACATATGATGCGATGTGC	cloning (*KS*)
KSrev	GCACATCGCATCATATGTCCACTCATGTATAACAGG	cloning (*KS*)
SKfor	CCTCTCATTCATGAGTGGACATATGATGCTATGTGC	cloning (*SK*)
SKrev	GCACATAGCATCATATGTCCACTCATGAATGAGAGG	cloning (*SK*)

Movie S1. **GFP:SYP132 localization in developing *sec1b keule* double mutant pollen**

References

1 Müller I*, et al.* (2003) Syntaxin specificity of cytokinesis in Arabidopsis. *Nat. Cell Biol.* 5:531-534.

2. Park M, Touihri S, Müller I, Mayer U, & Jürgens G (2012) Sec1/Munc18 protein stabilizes fusion-competent syntaxin for membrane fusion in Arabidopsis cytokinesis. *Dev. Cell* 22:989-1000.

3. Reichardt I*, et al.* (2011) Mechanisms of functional specificity among plasma-membrane syntaxins in Arabidopsis. *Traffic* 12(9):1269-1280.

4. Assaad FF, Huet Y, Mayer U, & Jürgens G (2001) The cytokinesis gene KEULE encodes a Sec1 protein that binds the syntaxin KNOLLE. *J. Cell Biol.* 152:531-543.

5. Karnahl M, Park M, Mayer U, Hiller U, & Jürgens G (2017) ER assembly of SNARE complexes mediating formation of partitioning membrane in Arabidopsis cytokinesis. *Elife* 6:e25327.

6. Lauber MH*, et al.* (1997) The Arabidopsis KNOLLE protein is a cytokinesis-specific syntaxin. *J. Cell Biol.* 139:1485-1493.

7. Park M*, et al.* (2017) Concerted action of evolutionarily ancient and novel SNARE complexes in flowering-plant cytokinesis. *Dev. Cell* 44:500-511.

8. Kwon C*, et al.* (2008) Co-option of a default secretory pathway for plant immune responses. *Nature* 451:835-840.

9. Heese M, Gansel X, Sticher L, Wick P, Grebe M, Granier F, & Jürgens G (2001) Functional characterization of the KNOLLE-interacting t-SNARE AtSNAP33 and its role in plant cytokinesis. *J. Cell Biol*. 155:239-249.

10. Sanderfoot AA, Kovaleva V, Bassham DC, & Raikhel NV (2001) Interactions between syntaxins identify at least five SNARE complexes within the Golgi/prevacuolar system of the Arabidopsis cell. *Mol. Biol. Cell* 12:3733-43.

11. Zheng H, Bednarek SY, Sanderfoot AA, Alonso J, Ecker JR, & Raikhel NV (2002) NPSN11 is a cell plate-associated SNARE protein that interacts with the syntaxin KNOLLE. *Plant Physiol.* 129:530-9.

12. Miller JH (1972) Assay of beta-galactosidase. *Experiments in Molecular Biology (CSH Laboratory Press, Cold Spring Harbor, New York, 1972*:p.352-355.

13. Misura et al., (2000) Three-dimensional structure of the neuronal-Sec1–syntaxin 1a complex. *Nature* 404:355-362.

14. Schmid M*, et al.* (2005) A gene expression map of Arabidopsis thaliana development. *Nat. Gene.t* 37:501-506.